Defects on silver based coatings

Mareška A., Kordová T., Míka M. H.
Department of Glass and Ceramics, University of Chemistry and Technology, Prague, Czech Republic
E-mail: mareskaa@vscht.cz

New trends in the automotive and construction industries are leading manufacturers to develop new materials with added value. In this article, we deal with the introduction of such a material, namely a silver-based emission coating, which is used in both architecture and the automotive industry. Silver--based coating thus makes it possible to increase the driver's comfort, or to increase the comfort of working in the office on hot steamy days. This coating changes the transmittance of IR radiation from or to the building, or from or to the car. The coating is based primarily on the presence of layers of silver, which are able to provide the primary functions of modulation of incoming and outgoing radiation. Silver-based coatings can also be used to heat, for example, car windshields. The production of a silver-based coating is very demanding and sensitive to the formation of coating defects. In this article, we discuss common coating defects and discuss their possible origins.

INTRODUCTION

When the emissivity of a window coating is low, the window coating is called low emissivity coating (low-e). Low-e coatings have been developed to minimize the amount of ultraviolet and infrared light that can pass through the glass without reducing the amount of visible light that is transmitted through the glass. There are two main types of low-e coating processes – pyrolytic low-e (also called online low-e), sometimes referred to as hard coating and magnetron sputtering vacuum deposition (MSVD), or "soft coating", which is used in both automotive and architectural industry. Silver-based coatings may contain varying amounts of silver layers. Coating with a triple layer of silver (Fig. 1), so-called offline low-e coating, is used in the automotive industry, for example for the production of automotive windshields. Low e coatings usually contain three layers of silver. The triple silver coating provides perfect heating performance and meets low-e limits. Coating with three layers of silver consists not only of three layers of silver, but also of other supporting layers, which ensure the final quality of the coated glass [1].

The electrical and optical properties of a silver-containing thin film strongly depend on the microstructure of silver, in particular on its crystal size, grain size, grain boundary size and surface roughness. The goal of low-e quality coatings is to improve the microstructure of thin silver to achieve optical optical quality and thermal performance [2-3].

Silver is most often sputtered on the so-called seed layer, most often consisting of zinc oxides, or tin dioxide, or other oxides. The task of the seed layer is to support the microstructure of the silver thin film. Among other things, this layer ensures that the optical and mechanical properties of the thin film are achieved. In addition, the zinc oxide seed layer can increase the size of silver crystals and increase its grain size, thereby reducing resistivity and absorption. Silver crystallizing in the (111) plane at the top of the basal ZnO (002) plane induces a lower resistivity than the polycrystalline Ag at the top of the zinc stannate. The ZnO crystal lattice supports the growth of silver in the (111) direction. The three silver atoms at the alternating quadruple hollow sites form the base cell (111) of the silver plane with a 2.6% lattice mismatch between the ZnO and Ag layers [4], Fig. 2.

The quality of the low-e coating is determined primarily by crystalline silver. The main task of the blocking layers is to prevent the oxidation of silver and

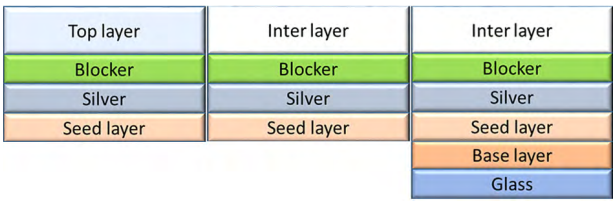


Fig. 1. Typical composition of Silver based coating with three Silver layers

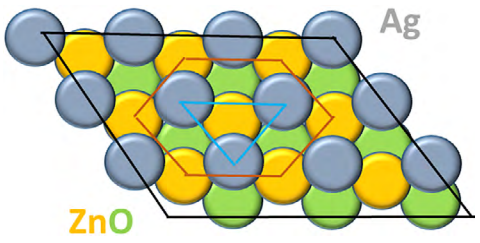


Fig. 2. Ag (111) growth atop of ZnO (002)

the diffusion of Ag^+ ions into the adjacent coating layers. The Ag film is so soft and unstable under oxygen plasma that it can oxidize or diffuse into adjacent layers while the oxide layers grow on the surface of the Ag film in an oxygen-filled chamber. This can result in deterioration of both optical properties and conductivity by the formation of mixed layers. A typical top layer, called a blocker, is made of oxide materials such as SnO_2, TiO_2 or ZnO. The optimized blocking layer consists of two parts: a metal part near the silver layer and an area with a higher oxidation ratio near the top layer. Typical blocker layer thickness is below 10 nm. A typical double E glass coating spectrum is shown in Fig. 3, with a transmittance of about 70% and a reflectance from the film and glass sides below 10% in the visible region. However, the transmittance in the IR region is close to zero ($\lambda > 1000$ nm) and the reflectance for IR is very high > 90% (for $\lambda >$ > 1000 nm). In addition, if three blocks of one silver are put together, IR selectivity and visibility are the best that can be achieved today [5-6].

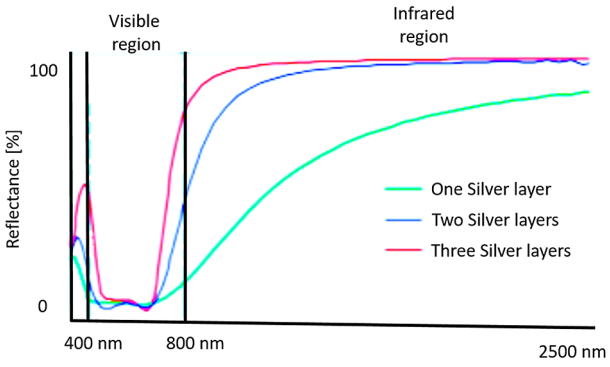


Fig. 3. Reflectance of glass based on the amoung of Silver layers

Production of the heated coated windshield begins on a float furnace. The float process (Fig. 4), invented by Sir Alastair Pilkington, dominates the flat glass industry so much that this technology produces virtually all glass panels in buildings and vehicles. Float flat glass thicknesses in the range of 0.5 to 20 mm are produced for various applications. In the case of laminated windshield, we most often talk about glass thicknesses from 1.6 mm to 2.1 mm.

The basic feedstocks for float glass production are soda, lime, sand, dolomite and sulphate and recycled shards. The presence of shards accelerates the melting process of raw materials and is an essential part of the incoming glass stem. As a result of the glass cullets presence, the energy consumption is limited and less CO_2 is emitted in the atmosphere. In the process of float glass on a float line, a homogeneous and well-homogenized inlet batch of glass is continuously transported to a place where the temperature is 1300 °C and where the molten glass is already present. The glass melts in the furnace at 1550-1600 °C. Melting occurs by heat transfer from the flames located above the glass surface. The direction of flames is reversed every 20 minutes to optimize the thermal balance in the furnace and the efficiency of the flue gases heat recovery chambers. The molten glass temperature is reduced from 1400 °C to 1100 °C in the last zone of the furnace before it enters the Tin bath. A cold air flow is regulated for it to presisely reach the temperature and the viscosity required in the forming zone. The conditioned glass melt flows into the bath of molten tin and forms a floating strip of glass, professionally called a glass ribbon. The temperature of the molten glass gradually decreases from 1100 °C to about 600 °C as it floats on the tin bath. The edges of the glass puddle are mastered by top rollers machines, which act on the spread surface of the glass. The top rollers effect, together with the exit speed of the ribbon are the two main factors to adjust its thickness and width. At a temperature of 600 °C, the glass ribbon leaves the tin bath. The glass is enough solid to climb on the metallic rollers and be driver inside the lehr. In the lehr zone, the glass is granually annealed to relax stress. Permanent stress is fixed in the region of temperatures from 480 °C to 600 °C. The glass reaches a certain value of compressive and tensile stress after controlled cooling, which allows its further processability in the process. The glass strip is withdrawn from the bath by rollers at a controlled speed. Different thicknesses are obtained by modulating the melt flow rate and the drawing rate of the cylinder. The glass ribbon is cooled down to the temperatures between 30 °C and 40 °C. The glass is cut afterthat into glass sheets and is placed on the stillages. The glass is ready to enter the next process [7].

In the following process called physical vapor deposition (PVD), the material is sputtered on the glass

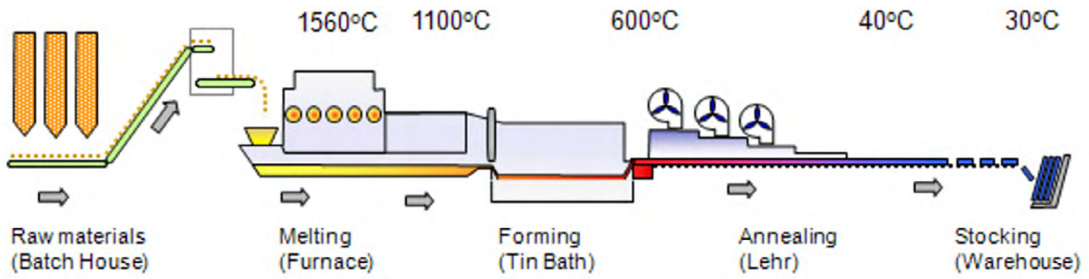


Fig. 4. Scheme of the float production line

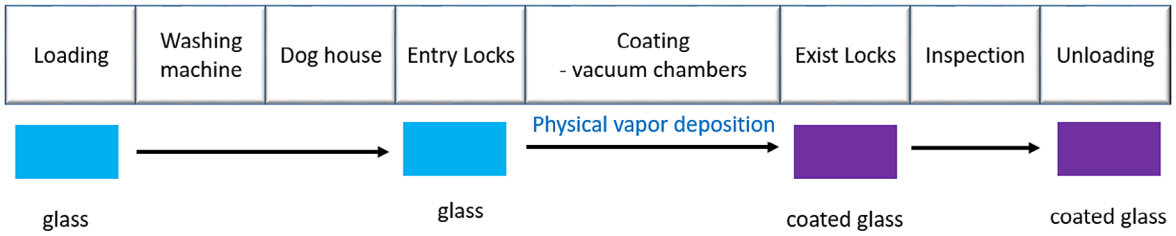


Fig. 5. Scheme of the physical vapour deposition production line

substrate in the vacuum chambers. The PVD process (Fig. 5) is the whole process from loading the glass substrate on the conveyor to placing it back on the pallet after the entire coating process has been completed. By glass substrate we mean glass coming from the float line. The arrangement of the coating depends on the composition of the coating itself. The length of the painting line depends on the composition of the coating itself - for example, the triple silver paint used for automotive purposes is much longer than the simple silver paint used for architectural purposes [8].

The glass sheet is roboticly loaded onto the line, by a manipulator. The robotic manipulator grabs the glass substrate by the suction cups and places it on the line. The glass is washed with high quality water, most often distilled water with low conductivity, less than 20 micro Siemens. Water purity is key to achieving optimal coating adhesion to glass. There must be no dirt left on the glass before the coating process in the vacuum chambers. The glass is dried, the remaining moisture on the glass surface is undesirable, ionization knives are also used for drying. The glass enters the so-called "dog house", which is a pressurized clean room that eliminates the deposition of impurities on the glass. The subsequent Entry lock consists of 3 chambers: buffer, hold and lock. By passing through the chambers, the glass substrate reaches the vacuum chamber, while the pressure in the chambers is constantly reduced until a vacuum is reached in the vacuum chamber (Fig. 6). The entry lock chamber cycles between atmospheric pressure and vacuum (760 torr to 20 mtorr). It consists of a chamber with slit valves to maintain the vacuum, rollers to transport the glass, pumps to create a vacuum and vent valves to return to atmospheric pressure. Entry hold is always under vacuum (<20 mtorr). It is pumped using diffusion pumps and cryogenic pumps. It is the last place where the glass can be stopped before it enters the coating chambers.

Entry buffer is always under high vacuum. It is pumped with diffusion pumps. The glass substrate load is converted from a batch flow to continuous flow through the coater through the use of the gap reduction rolls. The thin film of material is sputtered on the glass surface in the vacuum chambers. Different amount of layers can be sputtered on the glass substrate layer by layer. In the case of silver-based coatings, we are talking mainly about oxide materials such as zinc oxide, tin dioxide, titanium dioxide and layers of metallic silver and titanium. Different layers provide different coating properties. The basic function is provided by silver layers, which must be well protected to prevent undesired oxidation of silver to the ionic state [8-10].

The source of the thin film material is a planner or rotary sputtering target of metal ceramic or plastic. Air is continuosly removed by vacuum pumps to create vacuum with a value between 10-6 mbar. Argon gas is introduced continuosly to achieve a low pressure argon atmosphere. A magnet array inside the cylindrical target generate a magnetic field. Cooling water is used to dissipate the energy coming from the sputtering process. The targets are rotating so the material will be utilized uniformly A high voltage is applied to the target it created a plasma which is concentrated along the magnetic field. The plasma consists of metallic Argon, Argon ions and free electrons. Argon ionts (Ar^+) is created by electron impacts on the Argon atom. Sputtering target is negatively charged therefore the Ar^+ are attracted towards the surface of the target. The argon ions collide with the target and eject the target atoms from its surface. Argon ions do not distinguish between target ions and impurities. If the dirt is on the target, it will most likely be sprayed on the glass. Impurities can be incorporated into the thin film structure by this side effect, which can result in undesirable film thin film properties.

The exit locks consist of three chambers – buffer, hold and lock. They complement the entry lock system

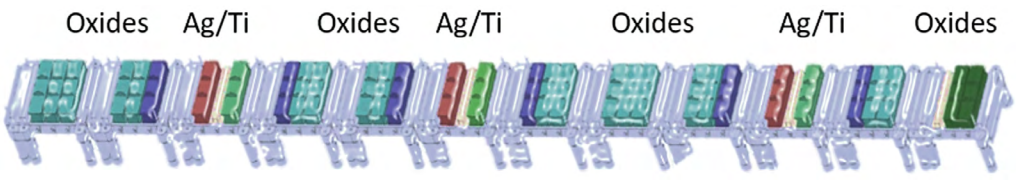


Fig. 6. Scheme of the vacuum chambers

and convert a continuous flow of glass into individual batches that can be cyclically removed from the coater. Coated glass is inspected online for defects and color. Rejections are marked and discarded. The glass sheets are lined with LDPE powder to prevent the glass sheets from sticking and to prevent mechanical damage to the sheets during transport in the pallet. The glass is ready for further operations, processing into a laminated glass front [8-10].

Coated glass enters another process line that can bend and laminate the coated glass together with the polyvinyl butyral interlayer into the final automotive laminated glass front. The tinted glass sheets are cut, then ground and then washed before a black or silver print is printed on them. The printed glass is pre-fired and then enters the bending furnace (Fig. 7), where it is shaped according to the shape requirements of the following processor, in this case the carmaker. The glasses bend either in the fifth on the kiln on pre-designed molds, ie the glasses get their shape thanks to gravity bending technology [11-12]. Another possible bending process is press bending, either from one or two sides, so-called single curvature bending or double curvature bending [13].

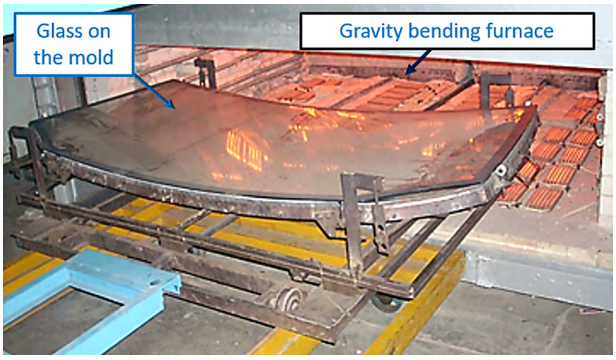


Fig. 7. Gravity bending technology of laminated windshield

During the assembly process, the two bent glass sheets are laminated together with the PVB interlayer (Fig. 8). Sandwich inner glass, polyvinyl butyral and outer glass are laminated using a pre-pressing furnace and an autoclave. The laminated glass is then inspected for aspect defects and in the next step other parts are glued to it [11].

The aim of this work is to analyze frequently occurring defects on silver based coating. In this work we solve the analysis of these defects using SEM-EDX and Raman spectroscopy and discuss possible sources in production where the defects could arise.

EXPERIMENTAL

Selection of coating defects

Samples provided by the laboratory processing coated glass are analysed by different laboratoring techniques and the root cause of the defects is discussed later on. Three different defects are selected (Fig. 9) as a top defects when depositing the coating in the laboratory of UCT Prague. Coat layers were deposited by physical vapor deposition in a vacuum chamber. A target with a defined material, which is applied to the substrate, glass, for a defined time, which is different for different layers, was used to deposit the coating. During the vapor deposition, a pressure of 10-4 Pa in the environment of magnet and plasma was achieved in the vacuum chamber.

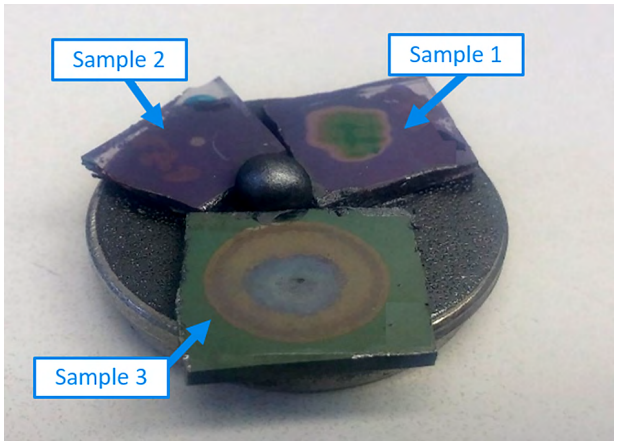


Fig. 9. Selected coating defects

SEM-EDX analysis

Defects are analyed using SEM-EDX analysis. SEM provides detailed high resolution images of the sample by rastering a focussed electron beam across the surface and detecting secondary or backscattered electron signal. An Energy Dispersive X-Ray Analyzer

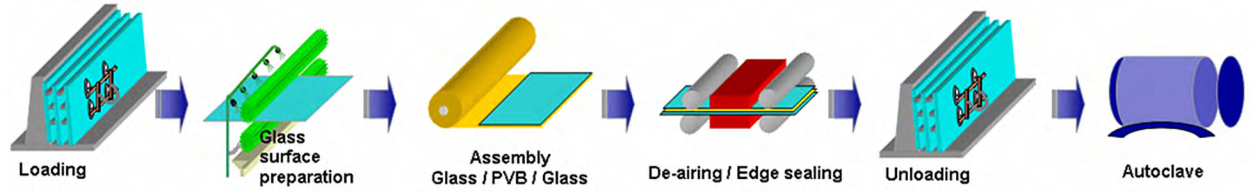


Fig. 8. Lamination of glass sheets with polyvinyl butyral interlayer

(EDX) is also used to provide elemental identification and quantitative compositional information. Hitachi SU8230 Regulus Ultra High-Resolution Field Emission SEM is used for the measurement. Hitachi device has an image resolution: 0.6 nm at 15 kV with the magnification range: 20× to 2,000,000×.

Raman spectroscopy

Raman spectroscopy is used to confirm possible presence of the organic contamination. Spectrometer Nicolet 6700 from the Thermo Scientific company with the measuring cell GladiATR (PIKE company) is used. DGTS detector is used. All spectrums are measured in the scale 4000 – 400 cm^{-1} with the resolution 4 cm^{-1} with 64 accumulated spectrums. Omnic 8.3 is used to analyze the spectrums.

RESULTS

Sample 1

Sample 1 is analyzed using SEM-EDX. First, the area not interfering with the site of the defect was analyzed (Fig. 10). The aim is to evaluate the chemical composition of the area.

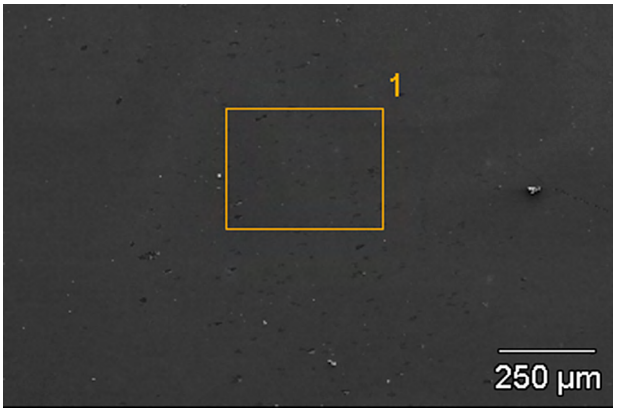


Fig. 10. Analysis of sample 1 – surrounding area

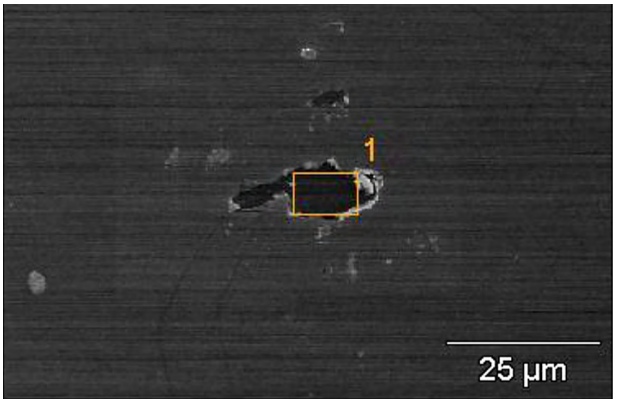


Fig. 11. Analysis of sample 1 – area of the defect

Subsequently, the chemical composition at the defect site is measured (Fig. 11). The size of the defect is 10 micrometers. The defect does not have a regular shape. There are several identical defects several units of micrometers in the vicinity of the main defect.

Both areas are compared in terms of chemical composition (Tab. 1). The main difference in the chemical composition lies in the presence of the elements Zinc, Titanium and Silver in the vicinity of the nearby defect. This fact indicates the presence of coating around the defect. Conversely, we detect a minimal amount of Zinc at the defect site compared to the defect-free site. At the same time, we detect no Silver or Titanium at the defect.

Tab. 1. Chemical composition in the defect area and in the surrouding area

Element	Surrounding area mass (%)	Defect area mass (%)
C	9.6	5.3
O	20.2	36.4
Mg	1.3	1.9
Al	0.3	0.1
Si	31.2	35.1
Ca	5.1	6.4
Ti	1.5	0.0
Zn	16.4	1.5
Ag	14.4	0.0
Na	0.0	13.4

No coating is identified at the defect site. This is probably a place where the coating is missing, technically called a pinhole. We detect -4.4 mass % points of Carbon, -1.5 mass % points of Titanium, -14.9 mass % points of Zinc and -14.4 mass % points of Silver in the defect area in compare with surrounding not defected are Fig. 12).

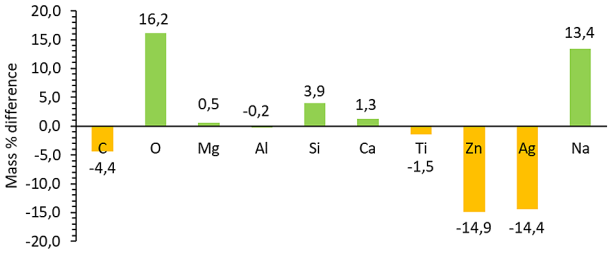


Fig. 12. Chemical comparison in the defect area and in the surrounding area – sample 1 – in percentage points (%)

Sample 2

Sample 2 is analyzed by SEM-EDX. We detect small formations located on the surface of the glass at the defect. The shapes have a spherical shape. There are

a large number of these point defects at the defect site (Fig. 13).

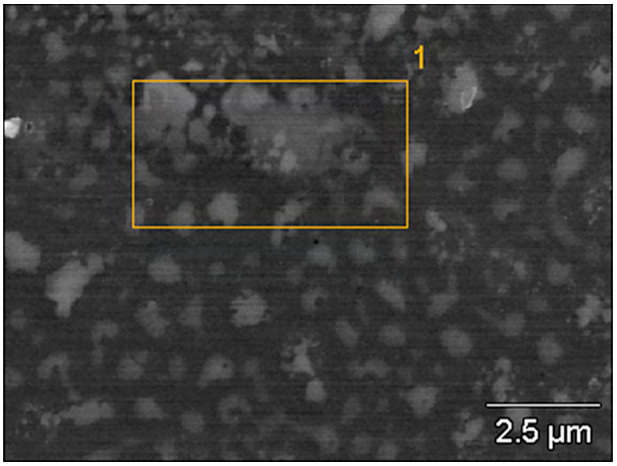


Fig. 13. Analysis of sample 2 – area of the defect

Subsequently, the sample 2 is focused so that it is possible to detect the chemical composition of one of the formations located on the glass surface. An increased amount of Silver is observed at the defect site compared to the surrounding glass. The defect is located on the surface of the glass and forms a spherical structure that is bounded.

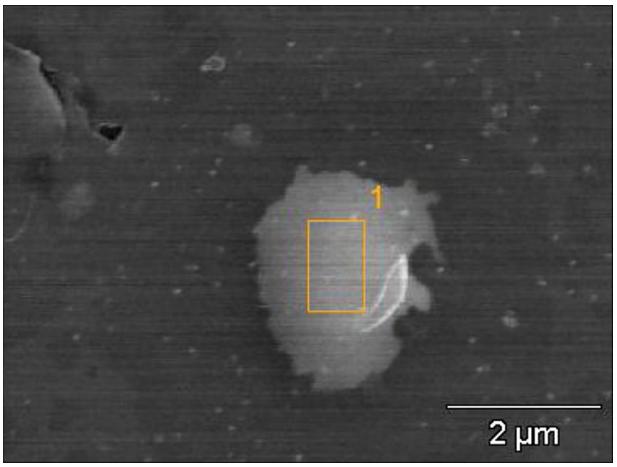


Fig. 14. Analysis of sample 2 – chemical composition of the defected unit

Both areas are compared in terms of chemical composition (Fig. 14, Tab. 2 and Fig. 15). The main difference in the chemical composition between the defect area and surrouding area lies in the higher amount of Silver and Tin in the defect unit.

Higher amount of Silver, Tin and Carbon is detected in the defected area. The defected area consists of different round units with the higher amount of Silver + 35.2 % points, + 11.4 % points of Tin and + 6.0 % points of Carbon in comparison with the surrounding area.

Tab. 2. Chemical composition in the defect area and in the surrouding area

Element	Defected area containing defect and surrounding area	Unit of the defect
O	25.8	11.2
Mg	1.4	0.0
Al	0.2	0.0
Si	30.5	9.0
Ca	5.0	0.0
Ti	1.7	0.8
Zn	15.7	6.6
Ag	19.7	54.9
C	0.0	6.0
Sn	0.0	11.4

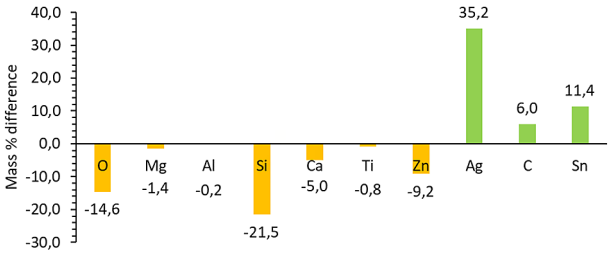


Fig. 15. Chemical comparison in the defect area and in the surrounding area – sample 2 – in percentage points

Sample 3

Sample number 3 with a defect is analyzed using SEM-EDX, where different defect sites are located. The defect is extensive and inhomogeneous throughout its surface. In Fig. 16 shows a given defect of 80 micrometers. The defect appears to be deep, most likely located partly on the glass surface and partly deep in the glass surface.

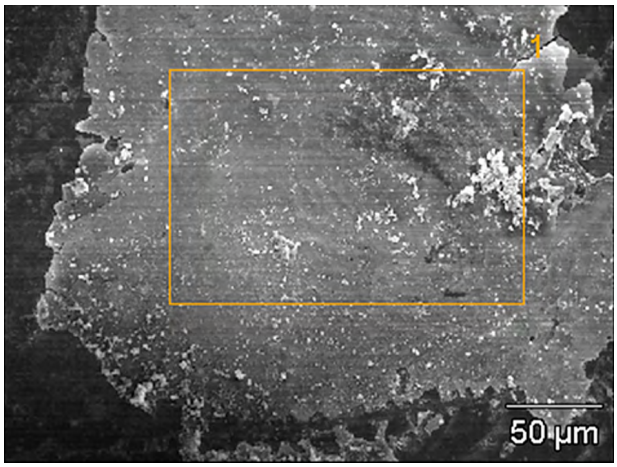


Fig. 16. Analysis of sample 3 – chemical composition of the defect

The defect boundary has the character of a skin peeling off the glass surface. Areas 1 and 2 in Fig. 17. In area 1 of Fig. 17 there is a kind of peeling shell of material, in area 2 there are some blisters of foreign material.

The defect on sample 3 is focused at the point where the foreign agglomerating material is detected (Fig. 18).

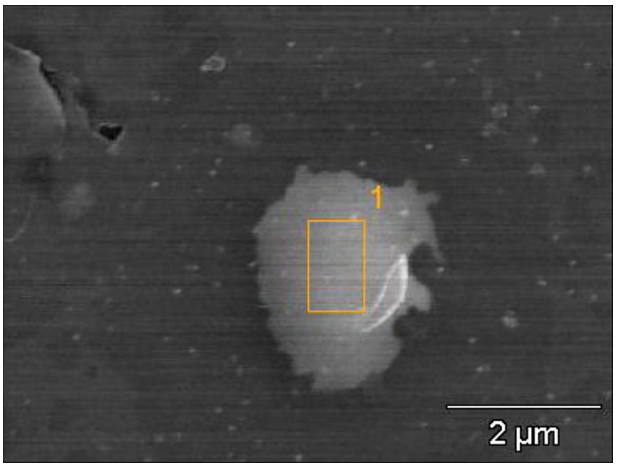


Fig. 17. Analysis of sample 3 – chemical composition of the defect – different areas 1, 2

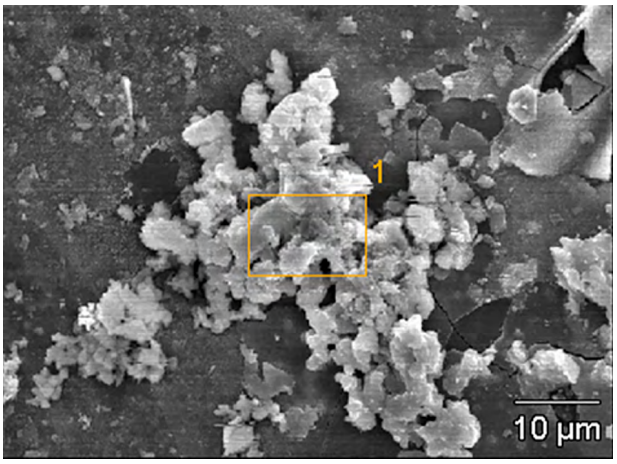


Fig. 18. Analysis of sample 3 – chemical composition of the defect – different areas 1

The different defect sites are compared in terms of the chemical composition of the foreign material at the defect site (Fig. 19). In Fig. 16 analyzes the first site that can be designated by its chemical composition as a representative chemical composition of the defect. At the analyzed site of sample 3 in Fig. 16 is detected 13.2 mass % points of Iron and 5.7 mass % points of Chlorine. Other contaminants appear to be Aluminum 0.3 mass % points and Nickel 0.7 mass % points.

In Fig. 17, two places are analyzed, namely area 1, where the peeling shell of the material whose chemical composition is analyzed is located. We detect 44.8 mass % points of Iron and 10.7 mass % points of Chlorine. We detect as well other contaminants like Copper in quantity 1.8 mass % points and Nickel in the amount of 0.9 mass % points . In area 2 and Fig. 17, where there are blisters of foreign material, we detect 29.9 mass % points of Iron and 8.1 mass % points of Chlorine. We detect as well other contaminants like Carbon 6.3 mass % points, Copper in quantity 1.0 mass % points, Nickel in the amoung of 1.1 mass % points and Aluminum in quantity 0.2 mass % points. In place 2 in Fig. 17, organic contamination of the glass at the defect site is probably detected due to the presence of a high amount of carbon, namely 6.3 mass % points.

In Fig. 18 we see crystallizing and agglomerating particles of foreign material with a chemical composition of foreign material of 38.9 mass % points of Iron, 9.6 mass % points of Chlorine. Furthermore, at the site of the defect is 0.2 mass % points of Aluminum, 3.8 mass % points of Nickel, 1.8 mass % points of Copper, 8.0 mass % points of Carbon, 1.1 mass % points of Sulfur and 0.9 mass % points of Manganese. The presence of carbon at the defect site in Fig. 16 confirms the previous presumption of the presence of foreign organic material. Based on the presence of various inorganic elements, we infer the presence of salts of organic material, such as carboxylic acid salts at the defect site. Raman spectroscopy is further used to confirm this assumption.

The Raman spectrum (Fig. 20) is performed with respect to possible contamination of the glass with organic matter before coating. OH-vibrations are visible in the range 3300-3600 cm^{-1}. Peaks in the range 1300-1500 cm^{-1}

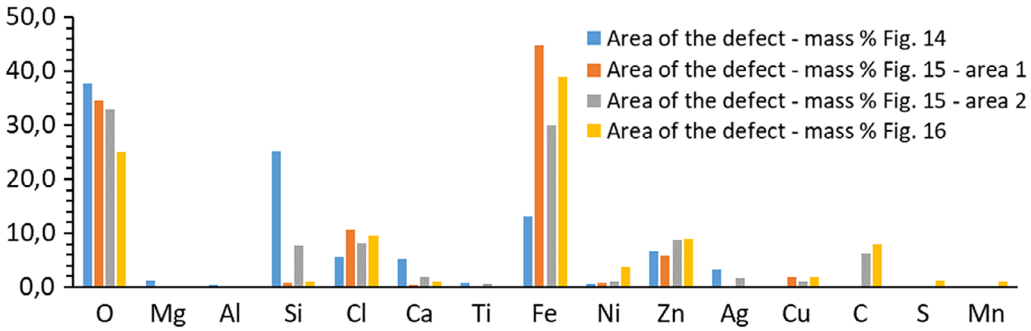


Fig. 19. Chemical composition in different areas of the defect located on the sample 3 in mass % points

relate to C bonds (COO-bonds). Organic contamination at the defect site is confirmed by Raman spectroscopy analysis.

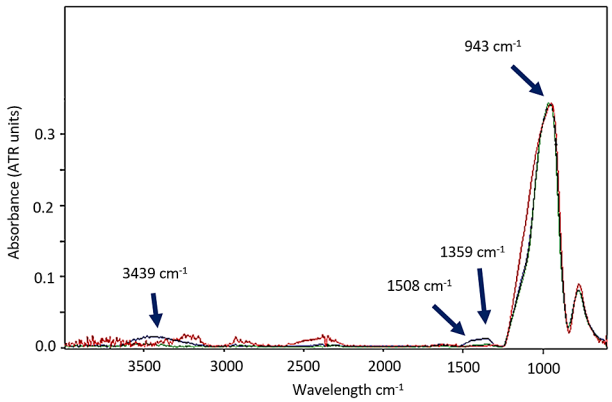


Fig. 20. Raman spectra of the defect on the sample 3 – different areas of the defect

DISCUSSION

The three defects found on the coated glasses are analyzed using SEM-EDX and Raman spectroscopy. The possible origin of the defect is being discussed.

The possible origin of the defect is determined. No contamination was found in the area of defect number 1. At the defect site, we observe that the coating is not localized. The surface of the glass is damaged, we can observe irregular grooves in the coating layer, referring to a defect caused during the processing of the coated glass. The defect can come from several parts of the process from coating to final glass processing. During the processing of the coating glass, it is necessary to prevent the slightest abrasion of the coating layer. Coated glass must always be transported on the non-coating side of the conveyor so that the coating layer is not damaged. The coating layer must not come into contact with foreign particles that could damage the coating layer, such as shards, oven brushes, or other sharp objects or contamination.

In the case of defect number 2, we can observe irregular formations on the top coat. This defect is visible to the eye and is always located on the top layer of the coating. When we focus more on the various formations on the glass, the formations are made of silver and tin, we can call these groups silver agglomerates. The inter-diffusion theory shows that silver ions diffused from the glass to the glass surface due to the presence of defects in the coating layers. Defects in the coating layers can occur, for example, due to the presence of contamination on the target during sputtering of the coating. Ion diffusion, on the other hand, occurs in an elevated temperature environment, such as a bending furnace, where ions diffuse from the coating to the glass surface and reverse ion diffusion (Na^+, H_3O^+ etc.) from the glass surface into the lower coating layers. Defects in the coating can also be caused by mechanical damage in the manufacturing process. Coating can be damaged, among other things, by scratching with a foreign object when processing coated glass [14-15].

Defect number 3 is a round defect, which is always found on the coated glass pane. We can observe damage to the coating in the defect area. The coated layer is partially delaminated. Contamination was found on the top glass layer. Contamination consists of Fe, Cl, Zn, Ni, Cu. The coated layer is partially delaminated. Due to the presence of organic contaminants (organic carbon), a Raman spectrum was performed with reference to contamination of the glass with oil/lubricant before coating. OH-vibrations are visible in the range 3300-3600 cm^{-1}. Peaks in the range 1300-1500 cm^{-1} refer to C bonds (COO– bonds). The glass must be clean enough to prevent contamination before painting. If there is any residual contamination on the glass and this contamination is covered, the coating may peel off in subsequent processes. The washing machine must be well maintained before painting. The conductivity of the water must be well controlled. Before painting, it is necessary to install a sophisticated filtration system on the washing machine.

CONCLUSIONS

Silver-based coatings are very popular materials in the architectural and automotive industries. From the point of view of processing, this material is very sensitive to the formation of defects, especially to mechanical damage and to the formation of defects in the coating layers. The critical steps to achieve a good quality product are the purity of the target during coating, the purity of the glass before coating and the prevention of mechanical damage to the glass in the processing process. Three surrogate defects are communicated in this article. The first defect refers to the absence of coating at the site of damage, it is a mechanical damage to the surface, thanks to which part of the coating is removed. The second defect refers to damage in the upper layers of the coating, which during heat treatment leads to the diffusion of silver and tin ions to the glass surface and to their agglomeration on the glass surface. The third defect is described as contaminated glass with organic and inorganic elements before coating. Contaminated glass is coated over the dirt. For this reason, there is a partial delamination of the coating at the location of the dirt. The article provides an overview of coating defects and discusses the possible causes of the defects and contributes to a faster solution of the problems in the process of coating glass processing.

Acknowledgement

I'd like to express my deepest thanks to my colleague Tereza Kordová for her contribution in this study. I'm extremely grateful to Martin Havlík Míka for his professional guidance, advice and for his contri-bution in this study.

REFERENCES

1. Nikitenkov N., Modern Technologies for Creating the Thin-film Systems and Coatings. IntechOpen: Moscow, **2017**; 418–420, doi 10.5772/63326.
2. Maschwitz P., Coster D., Decroupet D., Low emisivity coating with low solar heat gain coefficient, enhanced chemical and mechanical poperties and method of making the same. **2018**, EP1881893 (B1).
3. Jell B. P., Kalnaes S. E., Gao T., Low-emissivity materials for building applications: A state-of-the-art review and future research perspectives. *Energy and Buildings* **2015**, 96, 329 – 356. doi 10.1016/j.enbuild.2015.03.024.
4. Miyazaki M., Ando E., A low emissivity film. **1991**, EP 0698585A1. https://patents.google.com/patent/EP0698585A1/en. (*accessed June 1st 2022*)
5. Castaldo A., Ferrara M., Highly performing low emission sputtered coatings stable in air for energy saving glazing units. *SMARTCASE*, **2018**, https://www.researchgate.net/publication/325756672_Highly_performing_low_emission_sputtered_coatings_stable_in_air_for_energy_saving_ glazing_units. (*accessed June 1st 2022*)
6. Amirkhani S., Bahadori-Jahromi A., Mylona A., Godfrey P., Cook D., Impact of Low-E Window Films on Energy Consumption and CO_2 Emissions of an Existing UK Hotel Building. *Sustainability* **2019**, 11 (16), 4265. doi 10.3390/su11164265.
7. Pilkington L. Review lecture: The float glass process. *Proc Roy Soc Lond A*. **1969**, 314, 275-25. doi 10.1098/rspa.1969.0212.
8. Baptista A., Silva F., Porteiro J., Miguez J., Pinto G., Sputtering Physical Vapour Deposition (PVD) Coatings: A Critical Review on Process Improvement and Market Trend Demands. *Coatings* **2018**, 8 (11), 402. doi 10.3390/coatings8110402.
9. Rossnagel S. M., Thin film deposition with physical vapor deposition and related technologies. *Journal of Vacuum Science & Technology A* **2003**, 21, 74. doi 10.1116/1.1600450.
10. Moghaddam S. A., Mattsson M., Ameen A., Akander J., Da Silva M. G., Simoes N., Low-Emissivity Window Films as an Energy Retrofit Option for a Historical Stone Building in Cold Climate. *Energies* **2021**, 14 (22), 7854. doi 10.3390/en14227584.
11. Jun X., Yibing L., Manufacturing of Automotive Laminated Windshields, *Impact Behavior and Pedestrian Protection of Automotive Laminated Windshield*. *Springer* **2019**, 21-37.
12. Goodwin C. J., Ridealgh J. A., Cheetham K. J., Heat Treatable Coated Glass Pane. 2018, https://worldwide.espacenet.com/publicationDetails/biblio?FT=D&date=20181018&DB=EPODOC&CC=US&NR=2018297891A1. (*accessed June 1st 2022*)
13. Vakkuri E. Y., Kaonpää A., Salonen T., Nikkanen T., Method and furnace for bending glass sheets. **1992**, https://patents.google.com/patent/EP0592862A1. (*accessed June 1st 2022*)
14. Malecka J. K., Kelly P. J., West G., Clarke G. C. B., Ridealgh J. A., Almtoft K. P., Greer A. L., Barber Z. H., Investigation of Silver Diffusion in TiO_2/Ag/TiO_2 Coatings. *Acta materialia* **2014**, 66, 396-404, doi 10.1016/J.ACTAMAT.2013.11.030.
15. Satoshi T. Oxygen and silver diffusion into float glass. *Journal of Non-Crystalline Solids* **2006**, 352 (36), 3910–3913. doi 10.1016/j.jnoncrysol.2006.06.010.